

C55.13: NESS 62

NOAA TR NESS 62

A UNITED STATES
DEPARTMENT OF
COMMERCE
PUBLICATION

NOAA Technical Report NESS 62

U.S. DEPARTMENT OF COMMERCE
National Oceanic and Atmospheric Administration
National Environmental Satellite Service



Proposed Calibration Target For the Visible Channel of a Satellite Radiometer

K. L. COULSON
H. JACOBOWITZ



WASHINGTON, D.C.

October 1972

NOAA TECHNICAL REPORTS

National Environmental Satellite Service Series

The National Environmental Satellite Service (NESS) is responsible for the establishment and operation of the National Operational Meteorological Satellite System and of the environmental satellite systems of NOAA. The three principal Offices of NESS are Operations, Systems Engineering, and Research. The NOAA Technical Report NESS series is used by these Offices to facilitate early distribution of research results, data handling procedures, systems analyses, and other information of interest to NOAA organizations.

Publication of a Report in NOAA Technical Report NESS series will not preclude later publication in an expanded or modified form in scientific journals. NESS series of NOAA Technical Reports is a continuation of, and retains the consecutive numbering sequence of, the former series, ESSA Technical Report National Environmental Satellite Center (NESC), and of the earlier series, Weather Bureau Meteorological Satellite Laboratory (MSL) Report. Reports 1 to 57 are listed in publication NESC 56 of this series.

Reports 1 to 50 in the series are available from the National Technical Information Service, U.S. Department of Commerce, Sills Bldg., 5285 Port Royal Road, Springfield, Va. 22151. Price: \$3.00 paper copy; \$0.95 microfiche. Order by accession number, when given, at end of each entry. Beginning with 51, Reports are available through the Superintendent of Documents, U.S. Government Printing Office, Washington, D.C. 20402.

ESSA Technical Reports

- NESC 38. Angular Distribution of Solar Radiation Reflected from Clouds as Determined from TIROS IV Radiometer Measurements, I. Ruff, R. Koffler, S. Fritz, J. S. Winston, and P. K. Rao, March 1967. (PB 174 729)
- NESC 39. Motions in the Upper Troposphere as Revealed by Satellite Observed Cirrus Formation, H. McClure Johnson, October 1966. (PB 173 996)
- NESC 40. Cloud Measurements Using Aircraft Time-Lapse Photography, L. F. Whitney, Jr., and E. Paul McClain, April 1967. (PB 174 728)
- NESC 41. The SINAP Problem: Present Status and Future Prospects. Proceedings of a Conference held at the National Environmental Satellite Center, Suitland, Md., January 18-20, 1967, E. Paul McClain, Reporter, October 1967. (PB 176 570)
- NESC 42. Operational Processing of Low Resolution Infrared (LRIR) Data from ESSA Satellites, Louis Rubin, February 1968. (PB 178 123)
- NESC 43. Atlas of World Maps of Long-Wave Radiation and Albedo -- For Seasons and Months Based on Measurements from TIROS IV and TIROS VII, J. S. Winston and V. Ray Taylor, September 1967. (PB 176 569)
- NESC 44. Processing and Display Experiments Using Digitized ATS-1 Spin Scan Camera Data, M. B. Whitney, R. C. Doolittle, and B. Goddard, April 1968. (PB 178 424)
- NESC 45. The Nature of Intermediate-Scale Cloud Spirals, Linwood F. Whitney, Jr., and Leroy D. Herman, May 1968. (AD-673 681)
- NESC 46. Monthly and Seasonal Mean Global Charts of Brightness From ESSA 3 and ESSA 5 Digitized Pictures, February 1967-February 1968, V. Ray Taylor and Jay S. Winston, November 1968. (PB 180 717)
- NESC 47. A Polynomial Representation of Carbon Dioxide and Water Vapor Transmission, William L. Smith, February 1969. (PB-183 296)
- NESC 48. Statistical Estimation of the Atmosphere's Geopotential Height Distribution From Satellite Radiation Measurements, William L. Smith, February 1969. (PB 183 297)
- NESC 49. Synoptic/Dynamic Diagnosis of a Developing Low-Level Cyclone and Its Satellite-Viewed Cloud Patterns, Harold J. Brodrick and E. Paul McClain, May 1969. (PB 184 612)
- NESC 50. Estimating Maximum Wind Speed of Tropical Storms from High Resolution Infrared Data, L. F. Hubert, A. Timchalk, and S. Fritz, May 1969. (PB 184 611)
- NESC 51. Application of Meteorological Satellite Data in Analysis and Forecasting, R. K. Anderson, J. P. Ashman, F. Bittner, G. R. Farr, E. W. Ferguson, V. J. Oliver, and A. H. Smith, September 1969. (AD-697 033)
- NESC 52. Data Reduction Processes for Spinning Flat-Plate Satellite-Borne Radiometers, Torrence H. MacDonald, July 1970.
- NESC 53. Archiving and Climatological Applications of Meteorological Satellite Data, John A. Leese, Arthur L. Booth, and Frederick A. Godshall, July 1970. (COM-71-00076)
- NESC 54. Estimating Cloud Amount and Height From Satellite Infrared Radiation Data, P. Krishna Rao, July 1970. (PB-194 685)
- NESC 56. Time Longitude Sections of Tropical Cloudiness (December 1966-November 1967), J. M. Wallace, July 1970.

NOAA Technical Reports

- NESS 55. The Use of Satellite-Observed Cloud Patterns in Northern Hemisphere 500-mb Numerical Analysis, Roland E. Nagle and Christopher M. Hayden. April 1971.

(Continued inside back cover)



U.S. DEPARTMENT OF COMMERCE

Peter G. Peterson, Secretary

NATIONAL OCEANIC AND ATMOSPHERIC ADMINISTRATION

Robert M. White, Administrator

NATIONAL ENVIRONMENTAL SATELLITE SERVICE

David S. Johnson, Director

NOAA Technical Report NESS 62

Proposed Calibration Target for the Visible Channel of a Satellite Radiometer

K. L. COULSON

H. JACOBOWITZ

WASHINGTON, D.C.

OCTOBER 1972

UDC 551.507.362.2:551.508.21

551.5	Meteorology
.507	Instrument carriers
.362.2	Satellites
.508	Meteorological instruments
.21	Radiometers

CONTENTS

	Page
Introduction	1
Theoretical considerations	2
Case of a Rayleigh atmosphere	3
Case of a turbid atmosphere with ozone.	12
Required Measurements.	18
Measurements of the direct flux F_D at the surface	18
Measurements of global flux	21
Measurements of surface reflectance	21
Suggested instrumentation and observations	23
Instrumentation for routine operations.	23
Instrumentation for special measurements.	24
Auxiliary observations.	25
Discussion	25
References	27

LIST OF FIGURES

Figure 1.--Total optical thickness and optical thickness of the various components of the Elterman 1968 model of a turbid atmosphere at White Sands.	5
Figure 2.--Relative flux $F(-\mu_0)$ at White Sands at various solar zenith angles for a Rayleigh atmosphere.	5
Figure 3.--Relative flux F_d downward at the surface of White Sands for a Rayleigh atmosphere and various solar zenith angles.	6
Figure 4.--Relative flux $F_{D_s} + F_{d_s} + F_{D_s}'$ downward at the surface of White Sands for a Rayleigh atmosphere and various solar zenith angles.	7
Figure 5.--Spectral reflectance of a sample of white gypsum sand from New Mexico, as measured by Hovis (1971)	8

- Figure 6.--Total relative flux downward at the surface of White Sands for a Rayleigh atmosphere and various solar zenith angles. Arrows indicate relative flux incident at the top of the atmosphere 9
- Figure 7.--Total spectral flux of radiation incident at the surface of White Sands for a Rayleigh atmosphere and various zenith angles of the sun. 10
- Figure 8.--Intensity I_{gD} and $I_{gd} + I_S$ of solar radiation directed outward from the nadir direction at the top of a Rayleigh atmosphere over White Sands. 11
- Figure 9.--Total intensity of solar radiation directed outward from the top of a Rayleigh atmosphere over White Sands 12
- Figure 10.--Mean of 79 vertical profiles of the aerosol attenuation coefficient, compared to that of a Rayleigh model, for the atmosphere over White Sands (after Elterman 1968) 14
- Figure 11.--Fractional transmission of Elterman 1968 model of a clear atmosphere over White Sands as a function of wavelength for various zenith angles of the sun. A curve for the Rayleigh model at $\theta_0 = 0^\circ$ is given for comparison 15
- Figure 12.--Relative flux of the various components of solar radiation downward at White Sands for an aerosol atmosphere and various solar zenith angles. 16
- Figure 13.--Total relative flux of solar radiation downward at White Sands for various solar zenith angles. 17
- Figure 14.--Components of the relative intensity outward from the nadir direction at the top of a turbid atmosphere over White Sands for a solar zenith angle $\theta_0 = 0^\circ$ 19
- Figure 15.--Components of the relative intensity outward from the nadir direction at the top of a turbid atmosphere over White Sands for a solar zenith angle $\theta_0 = 60^\circ$ 19
- Figure 16.--Total absolute intensity outward from the nadir direction at the top of a turbid atmosphere over White Sands. (Incident flux as given by Thekaekara) 20
- Figure 17.--Bidirectional reflectance of white gypsum sand as a function of nadir angle in the principal plane for two different zenith angles of the source at a wavelength of $0.643\mu\text{m}$ (after Coulson 1965) 22

PROPOSED CALIBRATION TARGET FOR THE VISIBLE CHANNEL OF A
SATELLITE RADIOMETER

K. L. Coulson and H. Jacobowitz

National Environmental Satellite Service
National Oceanic and Atmospheric Administration
Washington, D. C.

ABSTRACT. A method is proposed for calibrating the visible channel of a satellite radiometer from orbit by using a sunlit area on the earth's surface as a calibration target. For a highly reflective surface and solar elevations of 30° or greater, the dominant component of the intensity of radiation directed outward from the top of the atmosphere is attributable to incident solar radiation which is transmitted directly downward through the atmosphere, reflected from the surface, and transmitted directly back out through the atmosphere. Aside from the solar constant, the only parameters that must be known to determine this dominant intensity component are the directional reflectance of the surface and the optical thickness of the atmosphere. Both can be measured directly with the proposed instrumentation. The intensity components arising from diffuse transmission or backscatter can be determined by measuring the global flux incident at the surface and applying radiative transfer theory for realistic models of the turbid atmosphere over the calibration site. A single filter instrument for the measurement of the global flux is suggested. A preliminary survey indicates that the white gypsum sand of the White Sands National Monument, N. Mex., may be the most suitable calibration target within the United States. If a suitable surface observation station could be established, another very attractive possibility is the Solar de Uyuni, a large salt flat at an altitude of 12,000 feet in Bolivia.

1. INTRODUCTION

Because there is no reliable on-board calibration for the visible channel of the ITOS scanning radiometer, there is a need for some method of calibration that can detect instrument changes following prelaunch calibration. One serious problem is the drift of instrument response with time, as observed with earlier radiometers. Another is the possibility that instrument properties are modified during the launch itself. Unless these changes are detected and appropriate corrections are applied, the data acquired in operations can

become unreliable and misleading.

Perhaps the simplest way to calibrate the instrument while it is in orbit is to use an area on the earth's surface as a calibration standard. Such a "standard surface", can be viewed repeatedly by the radiometer as the satellite passes over the selected area. By knowing the reflectance of the standard surface and the characteristics of the intervening atmosphere, it is possible, in principle, to compute the intensity of radiation directed to space from the standard surface to the satellite; thus the standard surface becomes a known calibration source from which instrument response can be determined. In practice, the problem is not so simple, mainly because of unknown atmospheric characteristics. However, by the method described below it should be possible to minimize these uncertainties to yield a reliable and reasonably accurate calibration source for the visible (and perhaps the near infrared) channel of the radiometer.

2. THEORETICAL CONSIDERATIONS

According to Coulson et al. (1965), the solar radiation returning to space from the top of the atmosphere consists of five separate components, each component having had its own transmission-reflection history in the atmosphere-surface system. The five components are described below. In the symbolic notation the subscript D indicates direct transmission and d indicates diffuse transmission; the first subscript is for the incoming radiation, the second for outgoing radiation.

Component No. 1: $I_{DD}(+\mu, \phi)$ - Radiation transmitted directly in its downward traverse of the atmosphere, reflected from the surface, and transmitted directly back out through the atmosphere. In general, the intensity is a vector quantity, but for an analysis of the energetics of the system, polarization effects can be reasonably neglected. In that case, I_{DD} is the scalar quantity (Coulson et al. 1965)

$$I_{DD}(+\mu, \phi) = \pi F_0 \mu_0 \rho(\mu, \phi; \mu_0, \phi_0) e^{-\tau(\mu + \mu_0)} \quad (1)$$

Here, μ_0 and μ are the cosines of the zenith angle θ_0 of the sun and the nadir angle θ of the upward radiation, respectively, ϕ_0 and ϕ are the corresponding azimuth angles, πF_0 is assumed to be the flux of solar radiation normal to the beam at the top of the atmosphere, ρ is the bi-directional reflectance of the surface, and τ is the normal optical thickness of the atmosphere.

Component No. 2: $I_{Dd}(+\mu, \phi)$ - Radiation transmitted directly through the atmosphere, reflected from the surface, and transmitted diffusely back out through the atmosphere. It is given in scalar form by the expression

$$I_{Dd}(+\mu, \phi) = \frac{\pi F_0 \mu_0}{4\pi\mu} e^{-\tau/\mu_0} \int_0^{2\pi} \int_0^1 \rho(\mu, \phi; \mu_0, \phi_0) T(\mu, \phi; \mu', \phi') d\mu' d\phi', \quad (2)$$

where $T(\mu, \phi; \mu', \phi')$ is the transmission function of the atmosphere (Chandrasekhar 1950).

Component No. 3: $I_{dD}(+\mu, \phi)$ - Radiation transmitted diffusely through the atmosphere, reflected from the surface, and transmitted directly back out

through the atmosphere. Methods of approximating this and the following components are discussed later.

Component No. 4: $I_{dd}(+\mu)$ - Radiation transmitted diffusely through the atmosphere, reflected from the surface, and transmitted diffusely back out through the atmosphere.

Component No. 5: $I_S(+\mu, \phi)$ - Radiation is backscattered by the atmosphere without ever having reached the surface. It can be expressed in the form

$$I_S(+\mu, \phi) = \frac{1}{4\pi\mu} S(\mu, \phi; \mu_0, \phi_0) \pi F_0 \quad , \quad (3)$$

where $S(\mu, \phi; \mu_0, \phi_0)$ is the reflection function of the atmosphere (Chandrasekhar 1950).

It is tempting to try to compute each of these components individually and thereby derive an intensity against which the radiometer could be calibrated. Our knowledge of atmospheric properties is still too meager, however, to obtain intensity values of sufficient accuracy and reliability for calibration purposes from theory alone. Thus it is proposed below that the theoretical calculations be bolstered by surface measurements to yield reliable and sufficiently accurate values of the outward intensity for radiometer calibration.

In general, the optical thickness τ , the transmission function T , and the reflection function S of the atmosphere are all dependent on the number, type, and spatial distribution of aerosols in the atmosphere. For a quantitative determination of the radiation available for calibrating the orbiting radiometer, the aerosol effects must be taken into account. This would present no great problem if the characteristics of the aerosols were known at the time of observation. Unfortunately, such knowledge is not generally available, so recourse to calculations based on aerosol models is necessary. Results for selected aerosol models are outlined in a subsequent section.

A. Case of a Rayleigh Atmosphere

As a preliminary step, consider the case of a Rayleigh atmosphere overlying a surface of white gypsum sand. Such a model should be a reasonably good approximation in the present problem for a number of reasons. First, the white gypsum sand exhibits a reflection pattern which is not strongly at variance with the Lambert case. Secondly, the aerosol content of the atmosphere of New Mexico is normally very low. Thus the Rayleigh approximation should not be too far from reality at White Sands, particularly for computations of the flux due to skylight. Finally, the skylight component is diffuse in character, thus minimizing directional effects at the surface, it constitutes only a small part of the total energy incident at the surface, and the effects of aerosols on the skylight would be only a small perturbation quantitatively.

The scheme is to find the total monochromatic global flux of radiation $F_g(-\mu)$ incident at the ground, reflect it from the white sand to get the outward intensity $I_g(+\mu)$ at the ground, transmit this intensity directly

and diffusely to the top of the atmosphere to obtain $I_{gD}(+\mu)$ and $I_{gd}(+\mu)$, and finally add the intensity $I_s(+\mu)$ due to backscattering of the original incident flux. Thus the total intensity from the nadir direction at the top of the atmosphere is

$$I(+\mu) = I_{gD}(+\mu) + I_{gd}(+\mu) + I_s(+\mu) \quad (4)$$

As discussed by Coulson (1968), the radiative flux $F_g(-\mu)$ incident on the ground consists of the following five components:

$F_D(-\mu_0)$: radiation transmitted directly through the atmosphere as the original parallel beam from the sun.

$F_{Ds}(-\mu)$: the part of $F_D(-\mu_0, \phi_0)$ reflected from the surface and backscattered by the overlying atmosphere in the first reflection-backscatter cycle.

$F_d(-\mu)$: radiation transmitted diffusely on its traverse of the atmosphere.

$F_{ds}(-\mu)$: the part of $F_d(-\mu)$ reflected from the surface and backscattered by the overlying atmosphere. This includes all orders of reflection-backscatter cycles of component $F_d(-\mu)$.

$F_{Ds}'(-\mu)$: a small flux due to all reflection-backscatter cycles of $F_D(-\mu_0)$ of order higher than the first.

Suscripts D and d indicate, respectively, the direct and diffuse transmission of the original incident radiation, and s indicates the scattering of the reflected radiation.

For the wavelengths of interest here ($0.5\mu m$ to $0.9\mu m$), $F_D(-\mu_0)$ is by far the largest. It is given by the simple exponential relation

$$F_D(-\mu_0) = \pi F_0 \mu_0 e^{-\tau/\mu_0} \quad (5)$$

where $\pi F_0 \mu_0$ is the monochromatic flux incident on a horizontal surface at the top of the atmosphere. Figure 1 shows the dependence of optical thickness on wavelength for the aerosol, Rayleigh, and ozone components of the atmosphere for the elevation of White Sands, interpolated from the tabulations of Elterman (1968). Computations of relative values of $F_D(-\mu_0)$ using the optical thickness of the Rayleigh atmosphere and the relation of (5), were made at intervals of $0.01\mu m$ from $\lambda = 0.5$ to $0.9\mu m$ for seven different zenith angles of the sun. The curves of figure 2 show the results. For these computations, F_0 has been set to unity. The fractional transmission of the Rayleigh atmosphere varied from 0.882 for $\lambda = 0.5$ to 0.988 for $\lambda = 0.9\mu m$ for the sun at the zenith. For a solar zenith angle of 60° , the corresponding values are 0.777 and 0.977.

Curves for component $F_d(-\mu)$, obtained by a double interpolation from the tabulation by Coulson (1968), are shown by figure 3. This component shows surprisingly little dependence on zenith angle of the sun, and it is quite small compared to the directly transmitted flux. In fact, for the sun at

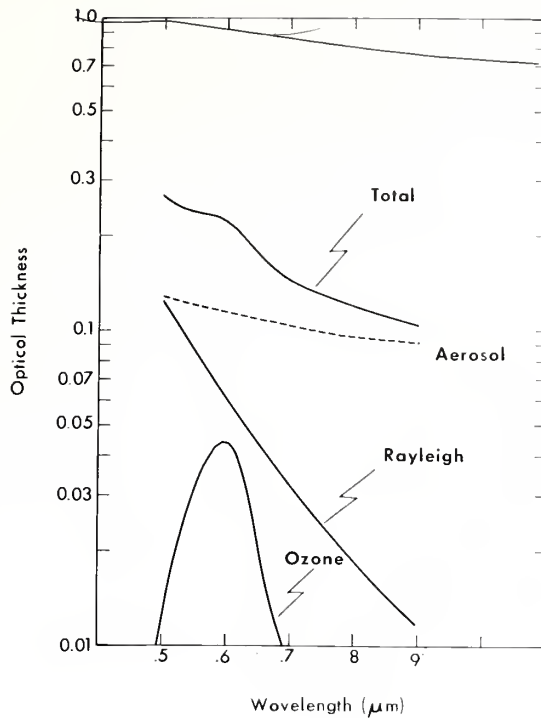


Figure 1. Total optical thickness and optical thickness of the various components of the Elterman 1968 model of a turbid atmosphere at White Sands.

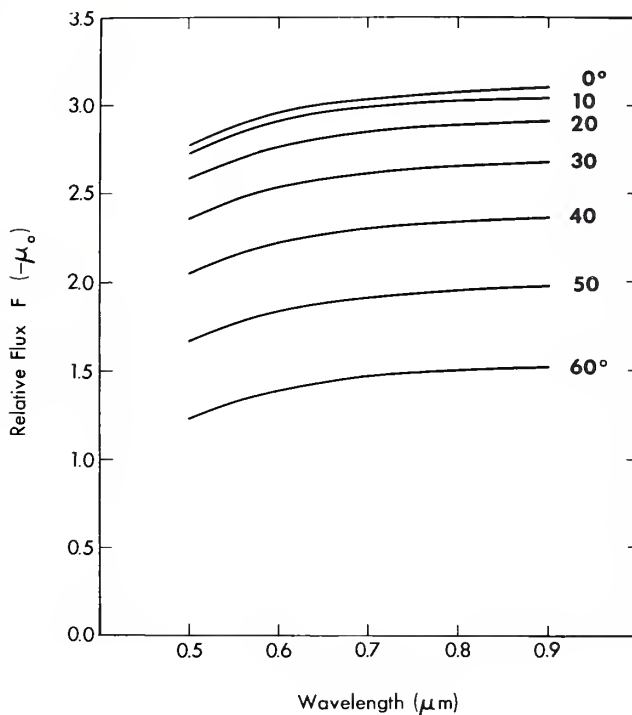


Figure 2. Relative flux $F(-\mu_0)$ at White Sands at various solar zenith angles for a Rayleigh atmosphere.

6.

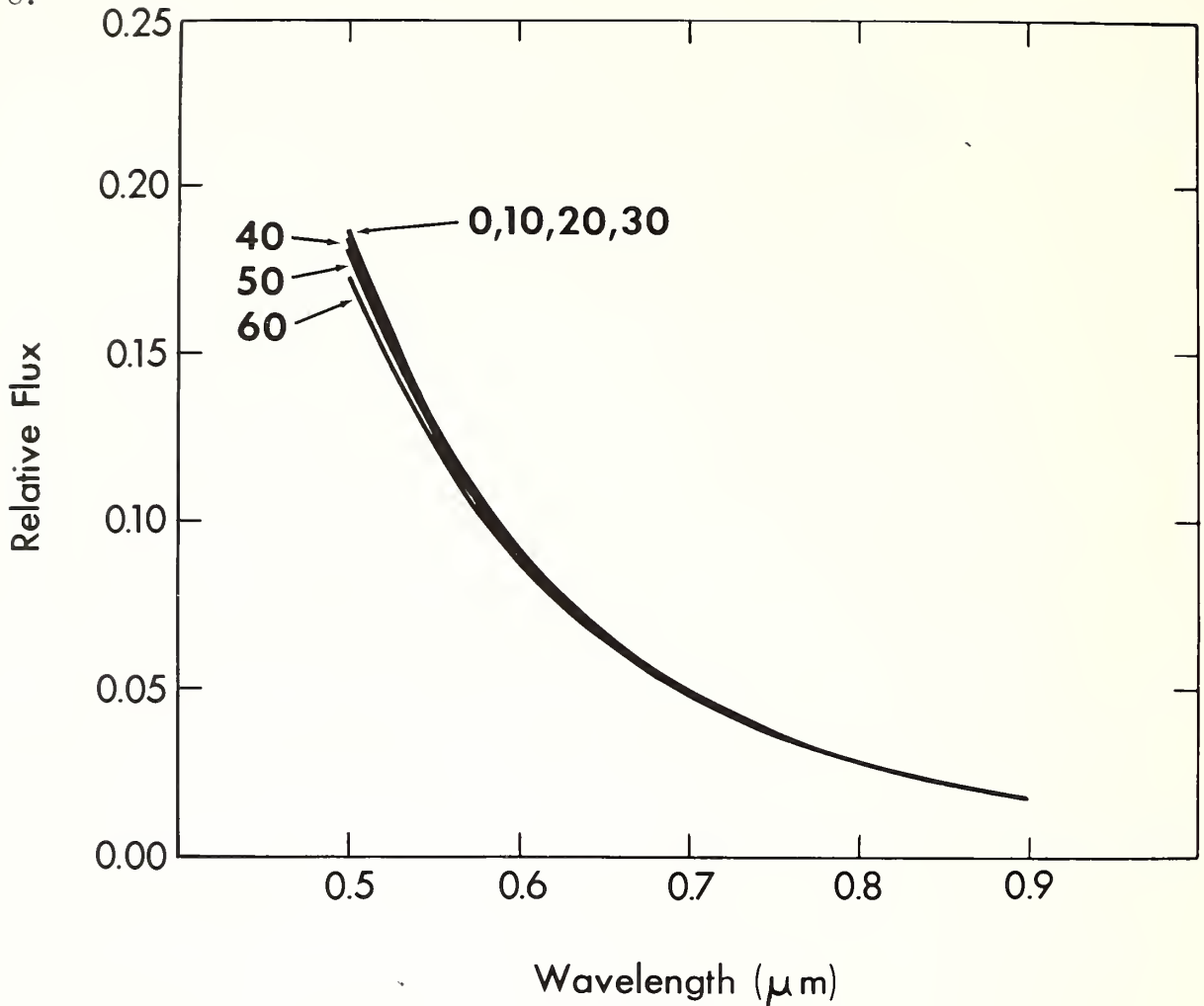


Figure 3.--Relative flux F_d downward at the surface of White Sands for a Rayleigh atmosphere and various solar zenith angles.

the zenith $F_D(-\mu)$ is only 6.8 percent of $F_D(-\mu_0)$ at $\lambda = 0.5$ m and 0.6 percent of $F_D(-\mu_0)$ at $\lambda = 0.9$ m. At $\theta_0 = 60^\circ$, the values increased to 14.3 percent and 1.2 percent, respectively.

The three components F_{Ds} , F_{ds} , and F_{Ds}^1 all arise because of the reflection and backscatter of the light incident on the surface. Their sum has been tabulated for selected parameters by Coulson (1968), from which the curves of figure 4 were obtained by multiple interpolation. The reflectance of the white gypsum sand (fig. 5) was taken as that measured by Hovis (1971). The magnitude of the sum $F_{Ds}(-\mu) + F_{ds}(-\mu)$ is of the same order as that of $F_d(-\mu)$ alone, a fact which means that backscatter of the surface-reflected radiation by the atmosphere results in the average intensity of skylight being approximately doubled because of reflection from the white sand surface.

Another interesting feature (shown in fig. 6) is that the flux incident at the surface is almost the same as that assumed incident at the top of the atmosphere. Physically, this means that the amount of energy lost to the

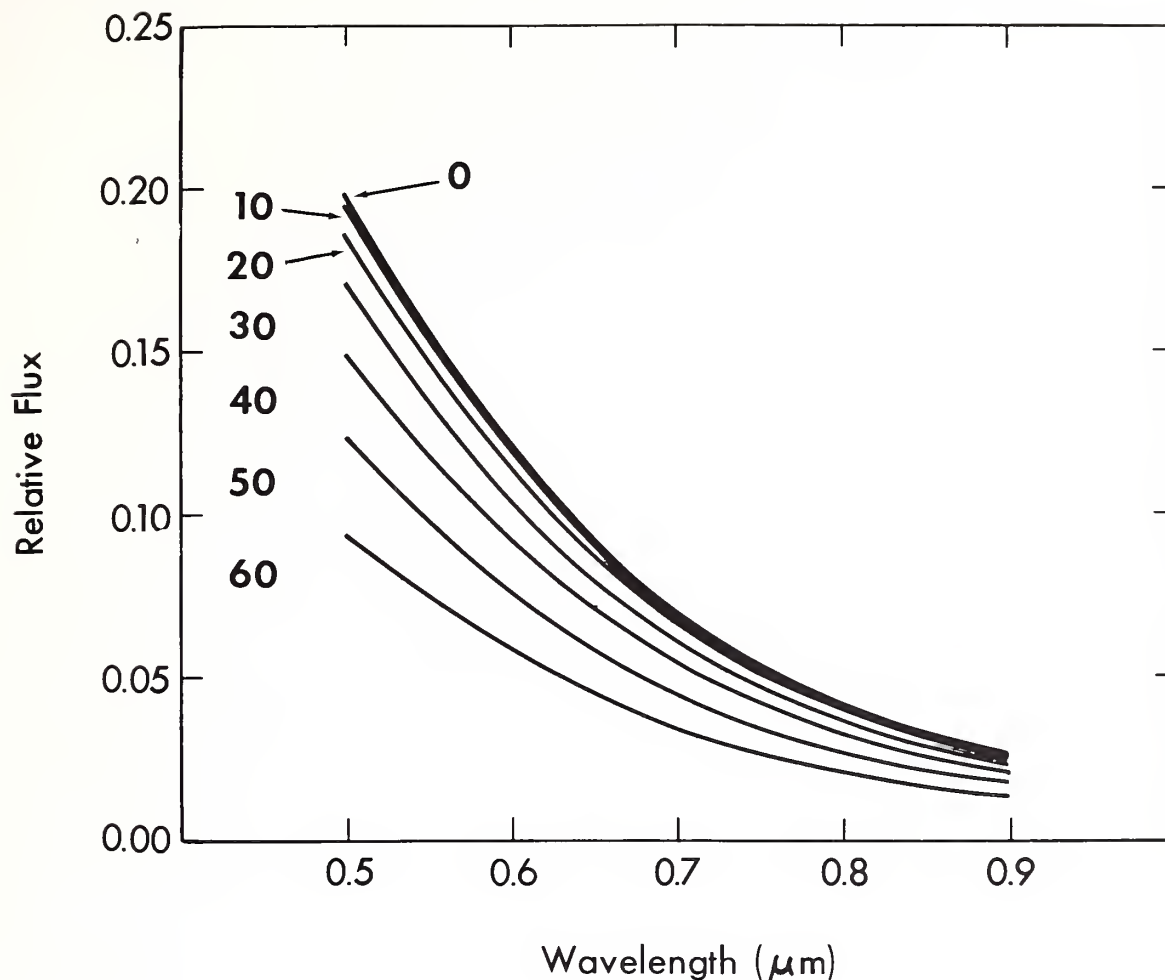


Figure 4.--Relative flux $F_{DS} + F_{ds} + F_{DS}'$ downward at the surface of White Sands for a Rayleigh atmosphere and various solar zenith angles.

system through being scattered back to space by the atmosphere is compensated for by part of the energy being directed back to the surface after single or multiple reflection by the white gypsum sand. (The atmosphere is assumed to be nonabsorbing.) Only for such a highly reflecting surface would so nearly complete compensation occur.

Changing the relative fluxes, shown so far, to absolute fluxes requires only a multiplication of the relative values by F_0/π (where F_0 is the absolute energy in the solar beam at the top of the atmosphere). The spectral distribution in absolute energy units of the total global flux $F_g(-\mu) = F_D(-\mu) + F_{DS}(-\mu) + F_{ds}(-\mu) + F_{DS}'(-\mu)$ incident at the surface at White Sands is shown for the case of a Rayleigh atmosphere in figure 7. Part of this energy combined with energy backscattered by the atmosphere itself is returned to the top of the atmosphere to yield the intensity field which might be used for calibrating satellite radiometers in orbit. The next task is to determine what the intensity of this outward radiation will be.

It is convenient to consider the outward radiation as consisting of the

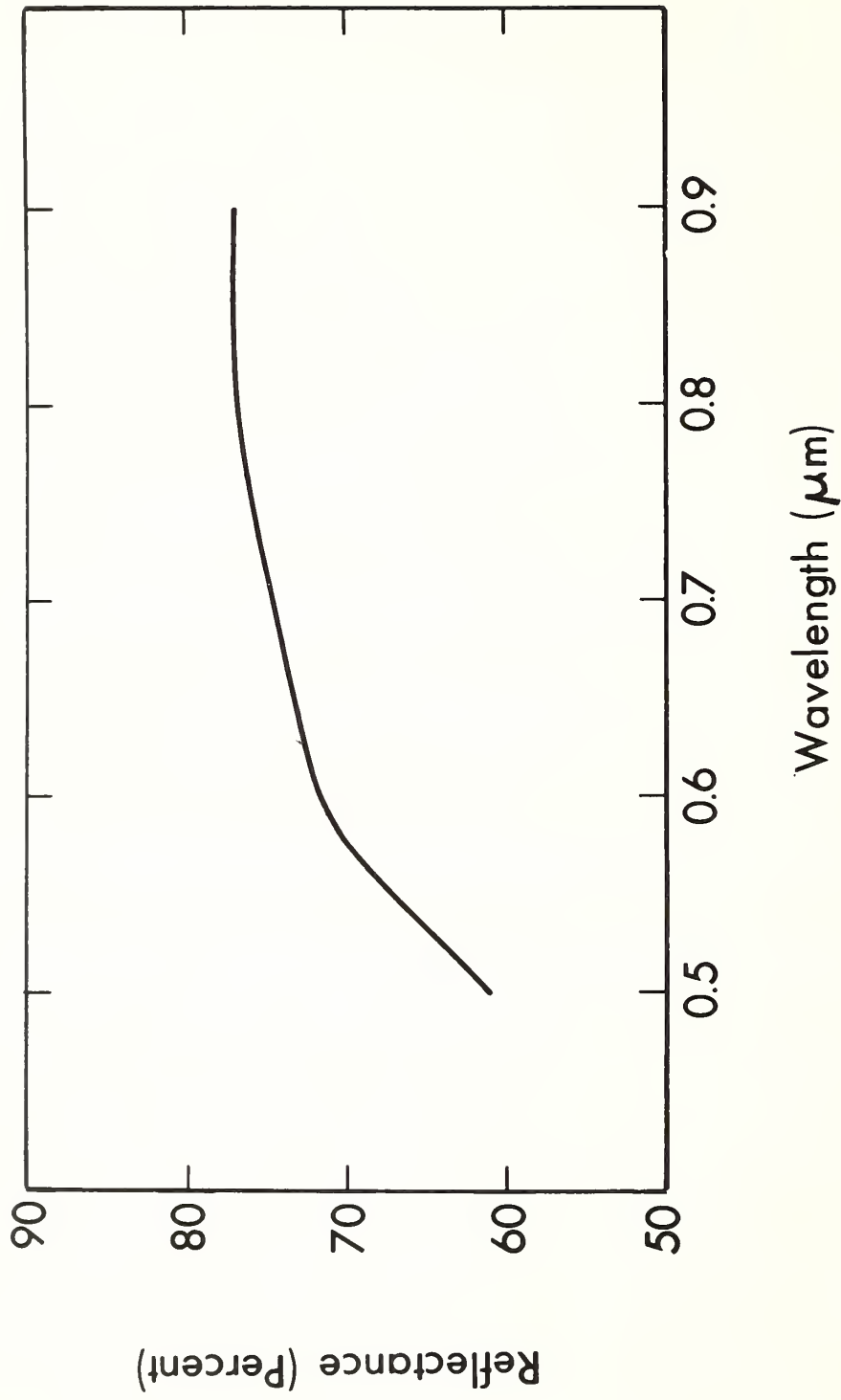


Figure 5.--Spectral reflectance of a sample of white gypsum sand from New Mexico, as measured by Hovis (1971).

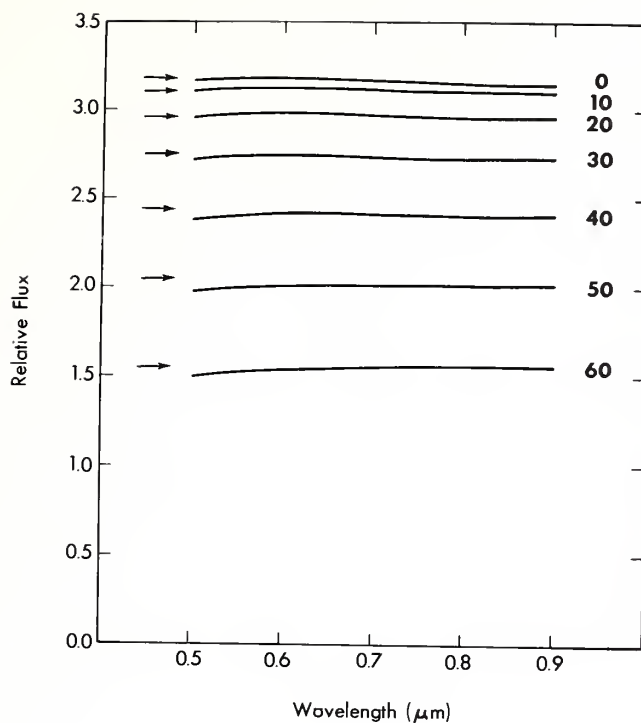


Figure 6.--Total relative flux downward at the surface of White Sands for a Rayleigh atmosphere and various solar zenith angles. Arrows indicate relative flux incident at the top of the atmosphere.

following three intensity components:

- $I_{gD}(+ \mu)$: surface-reflected radiation transmitted directly through the atmosphere.
- $I_{gd}(+ \mu)$: surface-reflected radiation transmitted diffusely outward through the atmosphere.
- $I_S(+ \mu)$: radiation backscattered by the atmosphere without having ever reached the surface.

We again assume, as a first approximation, a Rayleigh atmospheric model and further assume that the radiometer is viewing directly downward over the White Sands area. This latter assumption is by no means necessary, but is realistic for an orbiting satellite. Generalization to non-nadir directions will present no difficulty, if such is necessary.

The first requirement is to determine the intensity $I_g(+ \mu)$ in the outward direction at the ground. For the Lambert surface assumed, this intensity is independent of direction and is of magnitude

$$I_g(+ \mu) = \frac{R}{\pi} F_g(- \mu), \quad (6)$$

where R is total reflectance of the surface. Values of R and $F_g(- \mu)$ are

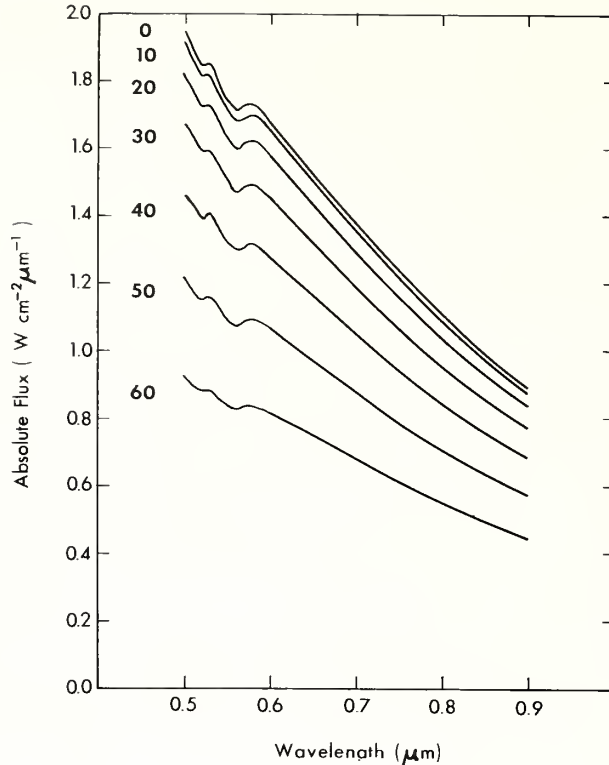


Fig. 7.--Total spectral flux of radiation incident at the surface of White Sands for a Rayleigh atmosphere and various zenith angles of the sun.

given in figures 5 and 7, respectively.

By far the most dominant component of the outward intensity for the case of White Sands is $I_{gD}(+)$. For the nadir direction it is expressed as

$$I_{gD}(+\mu) = I_g(+\mu)e^{-\tau} \quad (7)$$

Curves of $I_{gD}(+\mu)$ are shown as functions of wavelength for seven different solar zenith angles in the top section of figure 8. It should be noted that the units ($W \text{ cm}^{-2} \mu\text{m}^{-1} \text{ sr}^{-1}$) are those of intensity, not of flux.

Values of component $I_S(+\mu)$ can be obtained by triple interpolation from the tables of Coulson, Dave, and Sekera (1960) using the appropriate values of surface reflectance for White Sands and the variation of optical thickness with wavelength at the altitude of White Sands. The accuracy obtained by this procedure is not high, but $I_S(+\mu)$ is a small quantity compared to $I_{gD}(+\mu)$. The interpolation errors are of second order and probably negligible.

No equivalent set of calculations is available for determining directly the component $I_{gd}(+\mu)$, but it too is a small quantity at the wavelengths of interest, so any errors resulting from its approximation will be of minor significance. The calculations necessary to determine $I_{gd}(+\mu)$ precisely for

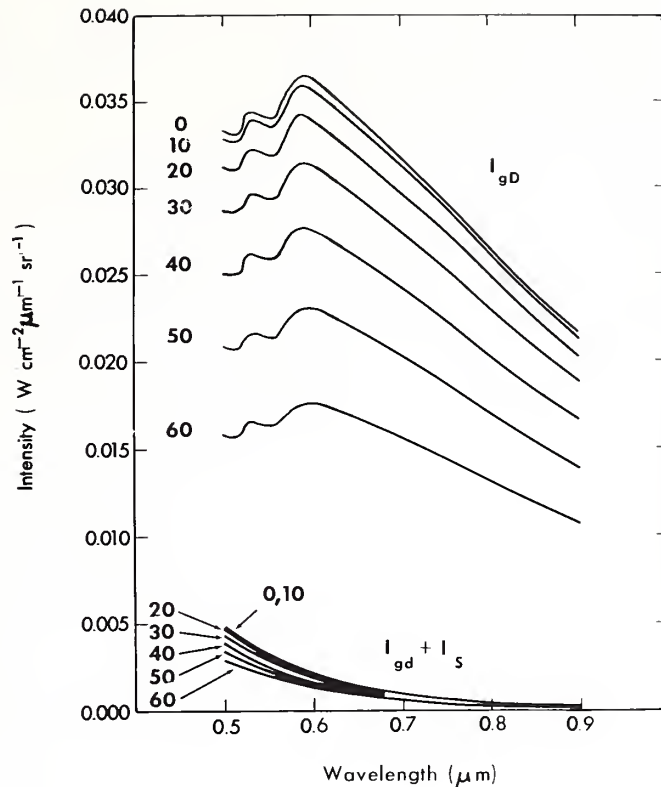


Figure 8.--Intensity I_{gD} and $I_{gD} + I_S$ of solar radiation directed outward from the nadir direction at the top of a Rayleigh atmosphere over White Sands.

a given atmospheric model are not difficult, but a suitable program is not immediately available. To use the tabulation of Coulson, Dave, and Sekera (1960) for the purpose, it was assumed that, because of diffuse transmission of reflected light, the emergent intensity from the nadir direction at the top of the atmosphere would be the same as the skylight intensity from the zenith direction at the bottom of the atmosphere for the same energy input. This should be completely valid by the reciprocity theorem (transfer characteristics invariant to exchange of incident and emergent directions) if the angular distribution of the two incident streams of radiation were the same. Such is not the case here; the sunlight incident at the top of the atmosphere is assumed to be monodirectional while that actually entering the base of the atmosphere after reflection from the surface is nearly isotropic. The worst possible error that could be introduced by this approximation is a factor of two, which would apply for a single scattering particle on which the two streams of incident radiation are normal to each other. The least possible error would be zero, which could occur at some specific intermediate angles of incidence of the monodirectional beam. The actual error from the approximation is between these two extremes. In view of the small inherent intensities involved, this error is probably negligible in comparison to those arising from the other assumption used.

The sum of the two components $I_S(+\mu)$ and $I_{gD}(+\mu)$ is plotted as a function

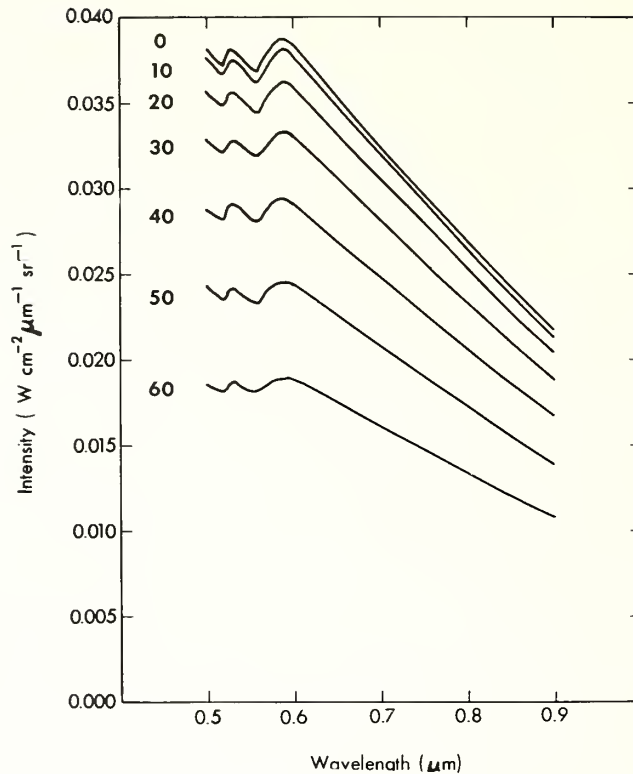


Figure 9.--Total intensity of solar radiation directed outward from the top of a Rayleigh atmosphere over White Sands.

of wavelength in the lower section of figure 8. A small extrapolation was necessary to extend the data of Coulson, Dave, and Sekera (1960) to wavelengths beyond $\lambda=0.8\mu\text{m}$. Figure 9 shows the total intensity of radiation emerging from the nadir direction for the model of Rayleigh atmosphere and Lambert surface over the White Sands area. This represents the maximum intensity that would be available for the calibration of orbiting satellite radiometers. Aerosol effects and the absorption by atmospheric ozone will tend to decrease the outward intensity from that obtained for the Rayleigh case.

B. Case of a Turbid Atmosphere With Ozone

The real atmosphere over White Sands always contains an aerosol component (dust, haze, smoke, and other types of particles) and some ozone. Characterizing these additional components is a serious problem in making a theoretical analysis of the radiative transfer that might exist at a given time at White Sands. The total amount of ozone is not known and, although the (Chappuis) absorption bands for ozone are relatively weak, they are broad and their cumulative effect is by no means negligible. Not only is there uncertainty about the aerosol content of the atmosphere, but optical properties, such as size-frequency distribution and index of refraction of the aerosols, are likewise still largely unknown. Thus, from a computation standpoint we are restricted to the use of models for determining logically what might occur. Even though models may reveal little about what actually occurs in a specific

case, the results of modeling are useful in setting limits on what might reasonably be expected.

A large number of atmospheric models are available from which to choose. The model chosen here is that of Elterman (1968). The main consideration for this choice is that it is based on 79 aerosol profiles obtained in the immediate area of White Sands by searchlight techniques. This model should represent atmospheric optical conditions over White Sands as validly as is feasible at the present time. In addition, the large number of measurements should permit the setting of some realistic limits on the variations to be expected.

The mean of 79 vertical profiles of the attenuation coefficient for the atmosphere over White Sands for $\lambda = 0.55 \mu m$ is shown in figure 10. The data were extrapolated from the level of the searchlight receiver (2.76 km) to sea level by assuming a scale height (height range required for a change in the coefficient by a factor of $1/e$) of 1.2 km. Since the surface of the white gypsum sand is at an altitude of 1.22 km, the largest attenuation coefficients near sea level are avoided. Still, aerosol attenuation in the model is considerably greater near the surface at White Sands than it would be for the Rayleigh atmosphere. The attenuation is comparable to the Rayleigh atmosphere throughout most of the middle and upper troposphere and stratosphere, and considerably lower in the region of the mesosphere.

The total ozone content of the atmospheric model of Elterman was set at 0.35 cm at standard temperature and pressure, a typical value for a mid-latitude station. However, the ozone content is quite variable over short time periods and seasonally. For accurate calculations for the satellite radiometer it would be desirable to use values measured at the time. According to D. Heath of NASA (private communication) total ozone content can be obtained to ± 5 percent accuracy from ultraviolet backscatter measurements from satellites, and from ozone measurements made routinely with a Dobson spectrometer in Colorado. Either source would be adequate for the purpose. If, however, as is suggested below, atmospheric attenuation is monitored continuously at White Sands for satellite calibration purposes, a knowledge of ozone content would not be necessary. Its effect would be taken into account implicitly in the surface measurements.

Turning now to a determination of the energy available for radiometer calibration in the case of the real turbid atmosphere over White Sands, we again discuss the various components of the radiation field at the surface and at the top of the atmosphere. It is well to remember for this purpose that the energy removed from a stream of radiation by attenuation is not necessarily lost to the radiation field. Attenuation is produced by both absorption and scattering. Absorption results in loss of radiant energy by conversion to some other form of energy; scattering simply produces a change of the direction of propagation of the energy. In the present problem, a considerable part of the energy from the original solar beam is scattered downward and still serves to illuminate the white sand at the surface. Likewise, part of the energy from the radiation directed outward is scattered upward and so can reach the radiometer.

The fractional transmission of the atmosphere is given by the exponential

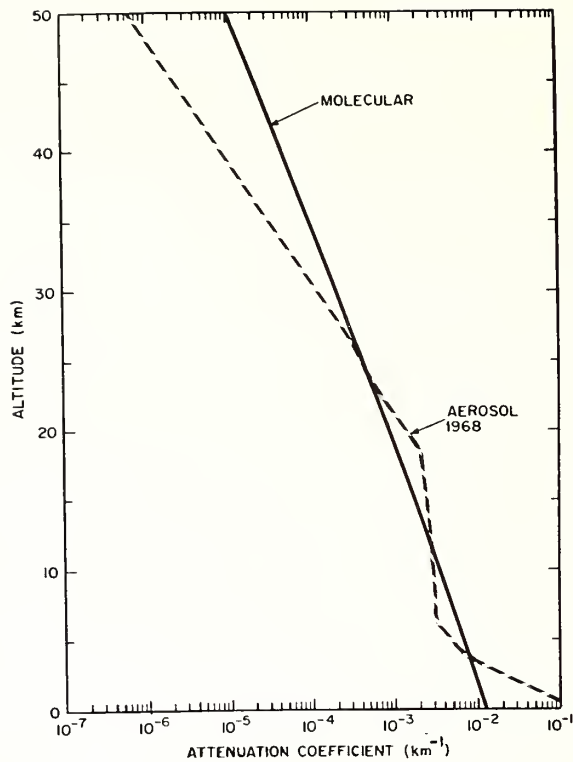


Figure 10.--Mean of 79 vertical profiles of the aerosol attenuation coefficient, compared to that of a Rayleigh model, for the atmosphere over White Sands (after Elterman 1968).

$T = e^{-\tau/\mu_0}$ for the optical thicknesses of the Elterman model, which includes all three components (aerosols, ozone, and Rayleigh particles). This is shown for various values of the solar zenith angle in figure 11. A curve for the Rayleigh atmosphere alone (at $\theta_0 = 0^\circ$) is included for comparison. Although the shapes of the curves are qualitatively similar, the curves for the turbid atmosphere show a transmission of roughly 10 percent less than that for the Rayleigh atmosphere. The dip in the curves in the 0.58 to $0.65 \mu\text{m}$ region is due to absorption by ozone.

The flux of direct solar radiation $F_D(-\mu_0)$ incident on a horizontal surface at the top of the atmosphere considering only the aerosol component is obtained by applying the equations of transfer to the aerosol component only. The results of computations for various solar zenith angles are shown in the top part of figure 12.

Determination of the diffuse radiation components is not so simple in the case of the turbid atmosphere. The problem of multiple scattering between aerosol particles and Rayleigh particles, and among the aerosol particles themselves, has never been solved in a completely satisfactory manner. In addition, a large expenditure of computer time is required for model calculations because of the complexities inherent in the Mie scattering theory.

The computation problem is somewhat alleviated if we neglect multiple scattering of radiation between aerosol particles and gaseous molecules, but still account for that among the gaseous molecules and aerosol particles.

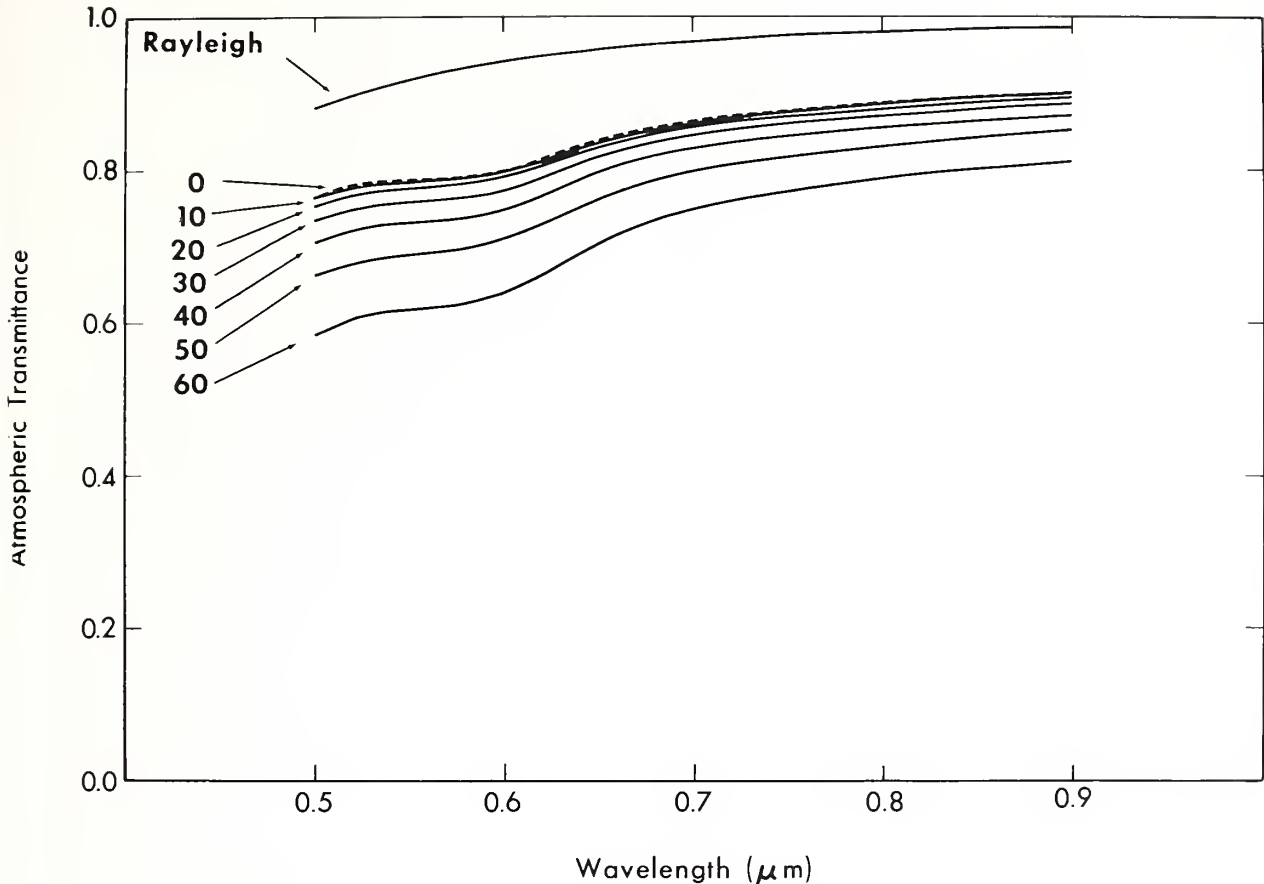


Figure 11.--Fractional transmission of Elterman 1968 model of a clear atmosphere over White Sands as a function of wavelength for various zenith angles of the sun. A curve for the Rayleigh model at $\theta_0 = 0^\circ$ is given for comparison.

This is a reasonable approximation for the atmosphere over White Sands, since the aerosol content of the atmosphere is quite low in that region. However, before the method is used for actual satellite calibration it would be well to account for complete multiple scattering of the radiation on both its downward and upward traverses of the atmosphere. It is possible to determine the total optical thickness of the atmosphere from measurements of the flux in the direct solar beam received at the surface, and from that to determine a reasonably accurate value of the total particle concentration for a representative size frequency distribution. This will permit the choice of one of a series of atmospheric models for which radiative computations need be performed only once.

For the present problem, we have chosen to compute the radiative fields for the aerosol atmosphere over White Sands by the matrix method of Twomey, Jacobowitz, and Howell (1966). This method is based on the doubling technique for multiple scattering calculations. By this method the radiative fields for an atmosphere of any desired optical thickness can be built up by computing the fields for a very thin layer for which single scattering calculations are a good approximation. The technique is repeated until the required optical

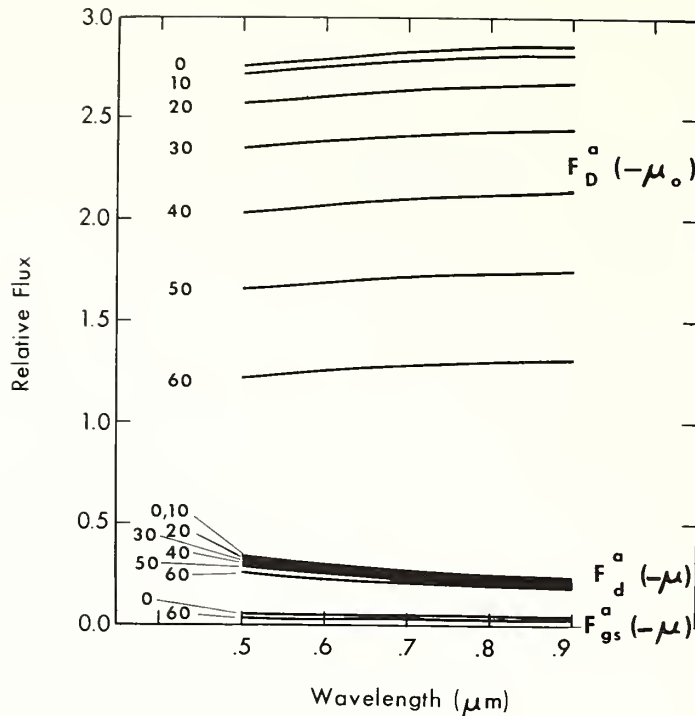


Figure 12.--Relative flux of the various components of solar radiation downward at White Sands for an aerosol atmosphere and various solar zenith angles.

thickness is achieved. The resulting field includes the effects of all orders of multiple scattering by the scattering centers of the medium. The size-frequency distribution of the aerosols was taken here to be the Junge distribution, with the exponent set at $\gamma = -4.0$ (Junge, 1952).

In principle, it should be possible to use the doubling technique to account for multiple scattering among all the particles of the medium, both aerosols and Rayleigh particles. The resulting field could be determined by a proper weighting of the contributions of scattering from a volume element of the medium, according to relative number density of the different particles and their respective phase functions. This more complicated method was not used in this exploratory study, but it would be advisable to use the additional precision attainable with the method for actual calibration of the satellite radiometer.

The fluxes $F_d^a(-\mu)$ and $F_{gs}^a(-\mu)$ due to diffuse transmission of the incident radiation and backscattering of the surface-reflected radiation by the aerosol component of the atmosphere were computed by the matrix method and are shown at the bottom of figure 12. Comparison of the curves for $F_d^a(-\mu)$ with the equivalent results for a Rayleigh atmosphere, given in figure 3, shows that the flux transmitted diffusely by the aerosols is considerably greater than that transmitted diffusely by the Rayleigh atmosphere, particularly at the longer wavelengths. This difference is a result of the different types of scattering phase functions for the different types of particles. Aerosol particles scatter predominantly into the forward direction, while the

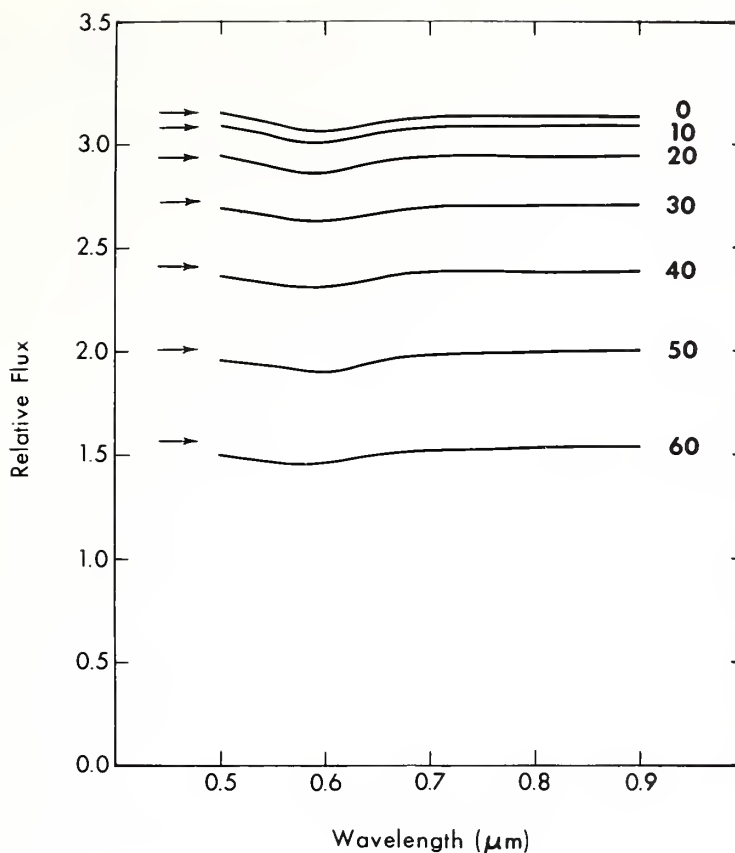


Figure 13.--Total relative flux of solar radiation downward at White Sands for various solar zenith angles.

scattering pattern for Rayleigh particles is symmetric for the forward and the backward directions. This difference in scattering patterns is responsible for the fact that the amount of surface-reflected radiation scattered back to the surface by the aerosol atmosphere is less than that scattered downward by the Rayleigh atmosphere (fig. 4).

A reasonably good approximation to the total flux incident at the surface of White Sands can now be obtained by adding together the components discussed above. The total flux downward at the surface is

$$F_g(-\mu) = F_D(-\mu) + \left[F_d(-\mu) + F_{gs}(-\mu) \right] R_+ \left[F_d^a(-\mu) + F_{gs}^a(-\mu) \right], \quad (8)$$

where superscripts R and a indicate Rayleigh and aerosol components, respectively. $F_D(-\mu_0)$ is computed from (5), with aerosols, Rayleigh particles, and ozone taken into account. The one element neglected is multiple scattering between aerosol and Rayleigh particles. Curves of the total relative flux incident at the surface for various zenith angles of the sun are shown in figure 13. The flux assumed incident at the top of the atmosphere for each zenith angle is indicated by an arrow. It is probable that absorption by ozone is responsible for the major part of the dip of the curves in the vicinity of $0.6\mu\text{m}$, even though a number of parameters are combined in defining the curves.

Because of lack of information on the bidirectional reflectance of the white sand surface, we assume that the intensity $I_g(+\mu)$, resulting from reflection of the flux $F_g(-\mu)$ incident on the surface is isotropic. Then we compute the radiation intensity from the nadir direction at the top of the atmosphere; this is the quantity that would be available for calibration of the satellite radiometer. As stated previously, this intensity consists of the following of components:

$$I(+\mu) = I_{gD}(+\mu) + \left[I_{gd}(+\mu) + I_s(+\mu) \right] R + \left[I_{gd}(+\mu) = I_s(+\mu) \right]^a \quad (9)$$

In the use of this equation, the total optical thickness of the turbid atmosphere is considered for the first term on the right and multiple scattering is accounted for by the quantities within each of the brackets. Cross terms between quantities within the brackets are neglected.

The relative contributions of the various components to the total intensity at the top of the atmosphere can be seen for $\theta_o = 0^\circ$ in figure 14 and $\theta = 60^\circ$ in figure 15. By far the major component in both cases, as well as in those not shown, is the intensity $I_{gD}(+\mu)$ resulting from direct upward transmission of the surface intensity $I_g(+\mu)$. For this component, only an attenuation of $I_g(+\mu)$ is involved; in computing this, the attenuation by aerosols, Rayleigh particles, and ozone is taken into account, so relatively high precision values are obtained for this major component. Computations of the other components are less precise, but their smaller magnitudes tend to decrease their relative contribution to the overall errors of the results.

We obtain the outward intensity in absolute energy units by multiplying the values of relative intensity at the top of the atmosphere (shown in fig. 14 and 15) by the quantity F_o/π , where F_o is the actual flux at the top of the atmosphere. This is the quantity we have been seeking for calibration of the satellite radiometer. The absolute intensities emitted outward from the nadir direction at the top of a turbid atmosphere over White Sands are shown for several different solar zenith angles in figure 16. The values of F_o as a function of wavelength were taken from Thekaekara (1970); these values have been adopted by the National Aeronautics and Space Administration for engineering design purposes. Note the spectral response of the radiometer to be calibrated in relation to the energy available. A typical transmission curve for the radiometer is shown in relative units in figure 16.

3. REQUIRED MEASUREMENTS

Valuable as model calculations are for putting the problem on a solid theoretical foundation, they are still no substitute for actual measurements. It is suggested that to provide a method for calibrating satellite radiometers using the White Sands area as a "standard surface", three types of measurements are necessary:

A. Measurements of the Direct Flux F_D at the Surface

Probably the largest source of error in the proposed calibration method is the lack of precise knowledge of all the atmospheric properties involved. As pointed out above, atmospheric particulates vary in type, amount, and

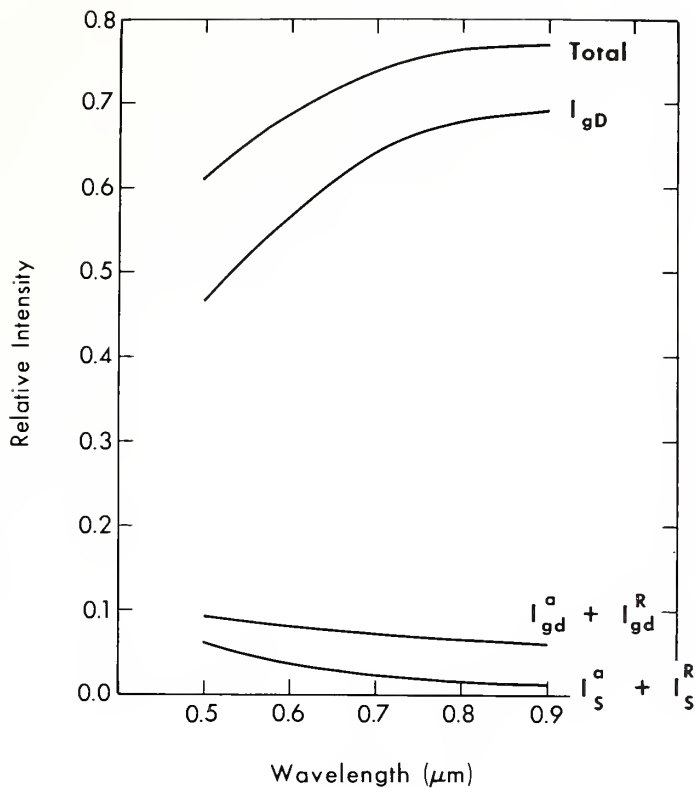


Figure 14.--Components of the relative intensity outward from the nadir direction at the top of a turbid atmosphere over White Sands for a solar zenith angle $\theta_0 = 0^\circ$

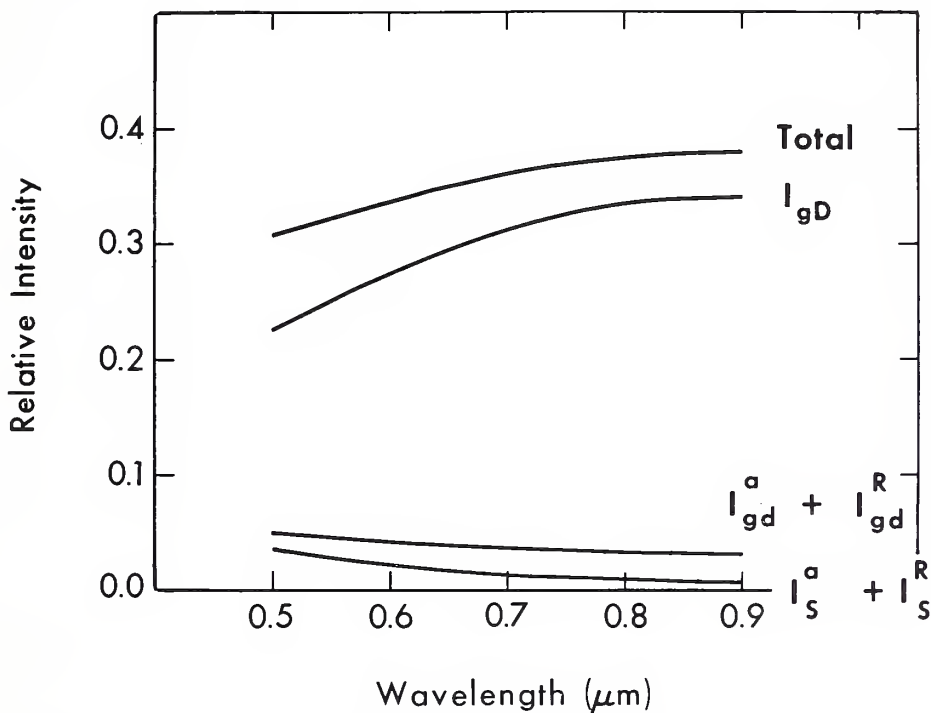


Figure 15.--Components of the relative intensity outward from the nadir direction at the top of a turbid atmosphere over White Sands for a solar zenith angle $\theta_0 = 60^\circ$

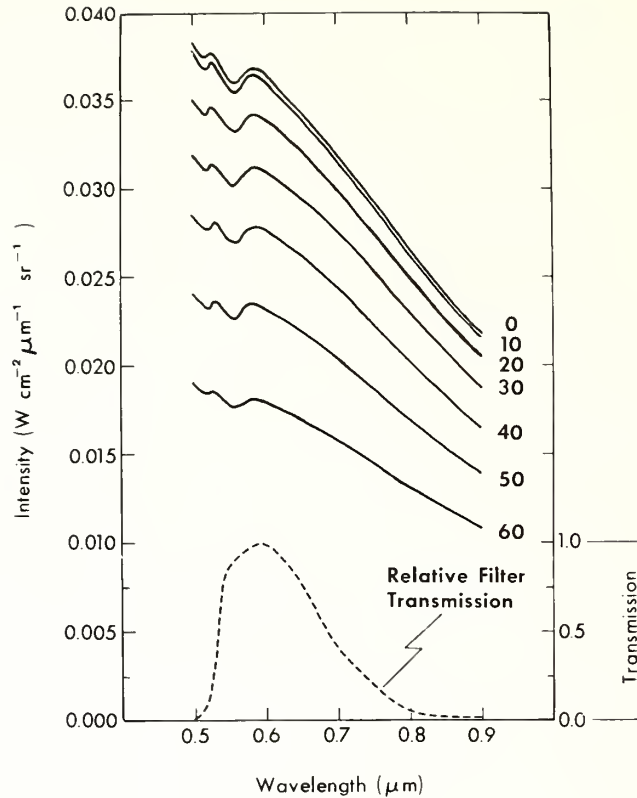


Figure 16.--Total absolute intensity outward from the nadir direction at the top of a turbid atmosphere over White Sands. (Incident flux as given by Thekaekara).

optical characteristics; the aerosol optical thickness generally is equal to or larger than that of the Rayleigh atmosphere in the 0.5 to 0.9 μm wavelength region, and the amount of ozone is variable with time and location. Measurements of the flux of the directly transmitted solar energy, $F_D(-\mu_0)$, can be used to derive corrections for these unknown atmospheric effects.

Figures 2, 3, and 4 show that the dominant source of energy incident on the surface at White Sands is the directly transmitted solar flux, $F_D(-\mu_0)$; figure 8 shows that the dominant intensity component from the nadir direction at the top of the atmosphere is $I_{gD}(+\mu)$, due to radiation which is transmitted directly upward through the atmosphere. To correct $I_{gD}(+\mu)$ for atmospheric effects at a given time, a determination of the atmospheric optical thickness τ can be derived from measurements of $F_D(-\mu_0)$. This value of τ can be used to correct the upward intensity $I_{gD}(+\mu)$ for atmospheric attenuation between the surface and the satellite. As an added bonus, the measurements of $F_D(-\mu_0)$ will serve as a check on measurements of global radiation incident at the surface.

The optical thickness of the atmosphere in the normal direction for the direct beam is simply

$$\tau = \mu_0 \ln \left(\frac{F_o(-\mu_0)}{F_D(-\mu_0)} \right) \quad (10)$$

where $F_0(-\mu_0)$ is known from solar constant determinations (Thekaekara, 1970), θ^0 is known from astronomical formulae (Robinson, 1966), and $F_D(-\mu_0)$ is measured. Then the intensity $I_{gD}(+\mu)$ in the nadir direction at the top of the atmosphere is

$$I_{gD}(+\mu) = I_g(+\mu)e^{-\tau} \quad (11)$$

B. Measurements of Global Flux

If the total global energy flux $F_g(-\mu)$ at the surface is known, the outward intensity $I_g(+\mu)$ can be determined for a Lambert surface by (6) written as

$$I_g(+\mu) = \frac{R}{\pi} F_g(-\mu) \quad (12)$$

If the surface is non-Lambert in character, then R/π must be replaced by a bidirectional reflectance $\rho(+\mu, -\mu_0, \phi_0)$, but otherwise the relation holds. Since the diffuse and direct radiation fluxes are both affected by atmospheric conditions, and the diffuse flux is not a unique function of atmospheric optical thickness τ , then it is necessary to measure $F_g(-\mu)$ at the White Sands surface.

C. Measurements of Surface Reflectance

There are a number of aspects of surface reflectance to be considered. First, we wish to know the extent to which the surface at White Sands is a Lambert surface. There are not enough measurements at the present time to determine this completely. The relatively few measurements available (Coulson, et al. 1965, Chen, et al. 1967, Salomonson 1968) show that the white gypsum sand approximates a Lambert surface more closely than any other natural surface for which measurements are available. For instance, from laboratory measurements, part of which are reproduced in figure 17, Coulson et al. (1965) found that for illumination from the direction of the surface normal, the relative reflectance ρ varied only about 6 percent as the direction of view varied from $\theta = 5^\circ$ to $\theta = 80^\circ$. However, for $\theta = 53^\circ$, ρ varied more than 25 percent for the same range of θ , and the curve is not symmetric around the nadir direction. Furthermore, the value of ρ in the nadir direction ($\theta=0^\circ$) increased from 66 percent for $\theta=0^\circ$ to 75 percent for $\theta=53^\circ$. Other measurements tend to corroborate these variations. Thus, one can conclude that total reflectance and bidirectional reflectance from the nadir direction are both relatively strong functions of angle of incidence for monodirectional radiation. This variation, which affects the determination of $I_g(+\mu)$, must be determined if the White Sands area is to be used for reasonably accurate calibration of the satellite radiometer. On the other hand, reflection of the diffuse fluxes $F_{DS}(-\mu)$, $F_{ds}(-\mu)$, $F'_{Ds}(-\mu)$, and $F'_d(-\mu)$ should be nearly isotropic over the hemisphere, but of course the magnitude of the first three must be dependent on the total reflectance.

An additional complication is introduced by the change of reflectance with wavelength. As was shown by figure 5, this is considerable in the sense that reflectance increases as wavelength increases from $\lambda = 0.5$ to $0.75 \mu m$. It is fortunate, however, that according to available measurements, the

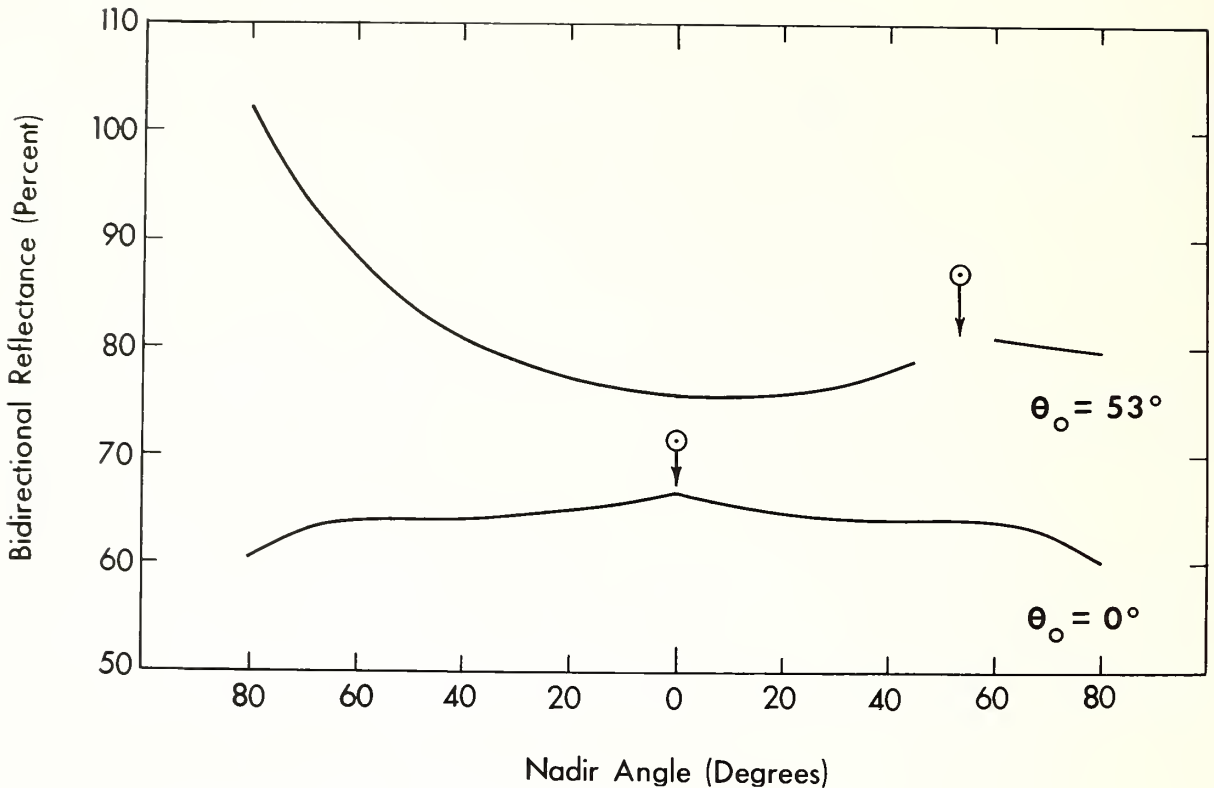


Figure 17.--Bidirectional reflectance of white gypsum sand as a function of nadir angle in the principal plane for two different zenith angles of the source at a wavelength of $0.643\mu\text{m}$ (after Coulson, 1965).

angular dependence of reflectance is nearly independent of wavelength; only the magnitude is wavelength dependent. This means that reflection data must be available at a number of wavelengths over the range of interest. It is not quite clear to what extent the curve of figure 5 will suffice to determine spectral dependence; it should be at least corroborated by in situ measurements.

Another source of concern is the possibility that reflectance of the white gypsum sand will change in time. On a time scale of years or decades, it is likely that any significant changes of reflectance of the White Sands area would be due to changes of vegetation. The gypsum sand itself is constantly being renewed by surface deposition through evaporation of mineral-laden water percolating from below, and winds blow the surface material about, thus exposing uncontaminated reflecting material. Thus, long-term changes must be of minor significance for this study. This is not necessarily so in the case of short-term changes, however. For instance, we do not know how the reflectance changes with changes in the amount of moisture present on the surface, nor whether the material is bleached by long exposure to sunlight. If either of these effects, or others, cause short-period changes of reflectance, the amount of the change should be monitored so appropriate corrections can be made. It is considered likely that only the total reflectance would be affected, and that the wavelength variation and directional dependence would remain unchanged, but this should be verified.

Finally, the reflectance characteristics of the White Sands region should be determined for low spatial resolution. The field of view of present satellite radiometers encompasses an area several kilometers across. Such an area in the White Sands region includes sand dunes, valleys, scattered vegetation, and other features. Measurements should be made to establish the directional reflectance of such large areas from the nadir as a function of solar zenith angle and wavelength. This could be a one-time determination by aircraft-mounted instrumentation. Because the accuracy of the calibration method is directly dependent on the accuracy of this one set of measurements, every effort should be made to assure reliability and the highest possible accuracy for this determination.

In summarizing the reflectance problem, we can state the following:

(1) For a determination of the outward intensity component $I_{gD}(+\mu)$ at the surface, both the direct flux $F_D(-\mu_0)$ and bidirectional reflectance $\rho(-\mu_0, \phi_0; \mu, \phi)$ must be known accurately. It was suggested above that $F_D(-\mu_0)$ be measured; here we add a suggestion that $\rho(+\mu, \phi; -\mu_0, \phi_0)$ from the nadir direction be determined for all zenith angles of the sun at which calibrations are likely to be performed.

(2) For a determination of the component of the intensity $I_g(+\mu)$ due to reflection of the diffuse incident light, the total reflectance $R(\mu_0)$ must be known for all solar zenith angles at which calibrations are to be performed. By knowing $R(\mu_0)$, it will be possible, with the Lambert assumption for only this part, to compute this flux component as

$$\left[F(-\mu) - F_D(-\mu_0) \right] \frac{R}{\pi} \quad (13)$$

where $F(-\mu)$ and $F_D(-\mu_0)$ are the flux components to be measured. The total outward intensity at the surface from the nadir direction becomes

$$I_g(+\mu) = \rho(1; -\mu_0) F_D(-\mu_0) + \left[F(-\mu) - F_D(-\mu_0) \right] \frac{R}{\mu} \quad (14)$$

(3) The total reflectance of the white sand surface should be monitored continuously to detect possible short-period changes of reflectance. If such changes do occur, measurements should be made to characterize any corresponding changes of spectral or angular distribution of the reflected radiations.

(4) The directional reflectance of the White Sands area should be determined as a function of wavelength and zenith angle of the sun. Spatial resolution should be similar to that of the satellite radiometer. Since the accuracy of the eventual calibration of the radiometer is directly dependent on the accuracy of this determination, the measurements should be of the highest possible accuracy and completeness.

4. SUGGESTED INSTRUMENTATION AND OBSERVATIONS

A. Instrumentation for Routine Operations

It is suggested that the equipment for routine operations at a surface station at White Sands consist of two radiation instruments and a two-pen strip chart recorder. The two instruments should be single-filter devices,

one a filter pyrliometer. The instrument designs might be similar to the following:

Filter pyrliometer - to measure the energy flux $F_D(-\mu_0)$ in the direct solar beam in the spectral interval of interest. The optical thickness of the atmosphere will be determined from this quantity. The device would be oriented toward the sun by means of a clock-driven equatorial mount. The field of view would be as small as feasible (perhaps a 2° half-angle cone), to decrease the amount of circumsolar radiation received. It is likely that the large changes of ambient temperature to which the instrument would be subjected and the high accuracy required will combine to demand complete temperature control of detector and associated electronics. Both instrument and mount must be adapted to a hostile environment. The instrument should be calibrated at least once every 6 months.

Filter pyranometer - to measure the global flux $F_g(-\mu)$ incident on the surface from the upward hemisphere and the global flux $F_g(+\mu)$ reflected from the white sand surface. The first of these is the basic measurement from which the large-scale outward flux will be determined; the second is for detecting possible short-period changes of surface reflectance by the ratio $F_g(+\mu)/F_g(-\mu)$. The most satisfactory receiver for both fluxes would seem to be an integrating sphere with the entrance aperture of the detector set into the side of it. The aperture would normally be in an upward-facing position to receive the downward radiation from sun and sky, yielding the flux $F_g(-\mu)$. It would occasionally be rotated to a downward-facing position to receive $F_g(+\mu)$, the upward radiation reflected from the surface. The rotation would be accomplished by mounting the instrument on a horizontal axis, around which the assembly could be rotated back and forth through a 180° angle on a preset program (perhaps 5 minutes of every hour) by an electric motor. The instrument would be located on a flat expanse of typical white sand at a height of 4 to 6 feet above the surface. The entire installation would have to be weather proof, the aperture of the sphere covered by an optical glass hemisphere, and the detector and electronics temperature controlled. Condensation of moisture on the glass hemisphere, always a problem in this device, would be minimized by providing temperature control or nitrogen flushing of the sphere. The system should be calibrated at least once every 6 months.

Strip-chart recorder - the two watchwords for the recorder are stability and reliability of operation. If the response of the recorder is stable it can be calibrated to yield accurate measurement data. Its operation must be reliable to minimize maintenance requirements and to yield continuous traces of impressed signals over long periods of time. Probably the most frequent problems of recorder operation are the inking of pens and the movement of the recorder chart. The recorder should be located in an air conditioned enclosure at a position sufficiently close to the receiving instruments to allow short transmission lines. It should be calibrated at least once every 6 months.

B. Instrumentation for Special Measurements

Aircraft-mounted radiometer - for determining the directional reflectance of the White Sands area, and the dependence of directional reflectance on zenith angle of the sun. If a new instrument were to be designed for this

purpose, it logically would be a single-filter instrument responding to the same wavelength range as that sensed by the satellite radiometer. It is likely, however, that existing instruments could be used for the purpose, either a duplicate of the satellite radiometer or the aircraft spectrometer of W. A. Hovis, NASA, Goddard. The choice would be that of the experimenter, but the measurements should be very accurate. One firm requirement is that they be made at a time when the surface instrumentation is in operation. They should be repeated at least once a year as a check on the entire calibration system.

C. Auxiliary Observations

A source of concern in the calibration of the satellite radiometer is the possible existence of clouds over the White Sands area at the time of the calibration. It may be possible to tell either from the satellite pictures or from the records of the surface instruments whether clouds were present, but visual observations by a weather observer would be valuable as corroborative evidence. Thus it is suggested that arrangements be made for weather observers of the U.S. Army weather station of the White Sands Missile Range to take special cloud observations at the times selected for calibration of the satellite radiometer.

5. DISCUSSION

In view of these considerations, the use of the White Sands area as a standard surface for the calibration of the visible channel of the satellite radiometer appears feasible, and the proposed method should permit derivation of a reasonably accurate absolute calibration of the instrument. In addition, the long-term stability of the surface at White Sands should yield calibrations essentially independent of time, from which trends of radiometer performance can be not only detected but corrected for quantitatively.

Attractive as the use of the White Sands area appears for the purpose, some thought should be given to the use of other areas. In the first place, the upward intensity over White Sands will be high and will thus give a high point on the calibration curve. Perhaps additional points are needed. It is likely that another calibration point, at a low intensity value, can be obtained by using space as a target. One or two well-defined points between these extremes would seem desirable.

One method of obtaining different intensities would be to use the White Sands area at different zenith angles of the sun. This might be feasible for an earth-synchronous satellite, but not for a sun-synchronous spacecraft. However, the errors due to atmospheric effects at larger solar zenith angles make more attractive the selection of an area with lower reflectance.

Various types of surfaces can be thought of as candidates. A water surface is known to have low reflectance at small zenith angles of the sun, and parts of the oceans are cloud-free a large percentage of the time. The main disadvantage of the sea surface as a target is that the reflectance may change with wind speed and particle content. Also, it would be difficult to put a surface observation station on the ocean to obtain ground truth data. A second set of possibilities is snow fields or glaciers, but features such as

variable reflectance, high-latitude locations, and large amounts of cloudiness over snow and ice fields decrease their attractiveness as calibration surfaces. A third possibility is some other land surface in subtropical desert areas, where the sun ranges over small zenith angles, cloudiness and precipitation are at a minimum, and an observation station can be established. This last approach seems to be the best of the three.

For a subtropical desert station one immediately thinks of the Middle East --the Sahara and the Arabian Desert. Satellite photographs show wide expanses of more or less uniform reflectance throughout the region which could be identified by means of prominent landmarks. One is faced, however, with establishing a surface observation station which would be reliable and which could be operated continuously. Without surface observations it is likely that errors introduced by unknown atmospheric properties would make any derived calibrations of questionable value. The feasibility of establishing a surface station at an oasis should be investigated.

One other site which looks attractive as a calibration surface is a dry lake bed on a high plateau of Bolivia. This area, the Salar de Uyuni, is a roughly circular salt flat about 60 miles diameter. It has an elevation of 12,000 feet and is located at about latitude 20°S . It shows up well on satellite photographs and appears to be relatively uniform in brightness. Its high altitude, low latitude, small amount of cloudiness, and lack of large sources of pollution all indicate that the area would be ideal for calibration purposes. Further investigation is needed as to the actual homogeneity of the surface and the feasibility of establishing a surface observation station at the site.

6. REFERENCES

- Chandrasekhar, S., Radiative Transfer, Oxford, Clarendon Press, 1950, 393 pp.
- Chen, H.S., Rao, C.R.N., and Sekera, Z., "Investigations of the Polarization of Light Reflected by Natural Surfaces," Scientific Report No. 2, Contr. AF 19(628)-3850, University of California, Los Angeles, 1967, 96 pp.
- Coulson, K.L., Dave, J.V., and Sekera, Z., Tables Related to Radiation Emerging from a Planetary Atmosphere with Rayleigh Scattering, University of California Press, Berkeley, 1960, 548 pp.
- Coulson, K.L., Bouricius, G.M., and Gray, E.L., "Effects of Surface Reflection on Radiation Emerging from the Top of a Planetary Atmosphere," T.I.S. Report R65SD64, Space Sciences Laboratory, General Electric Co., Philadelphia, 1965, 149 pp.
- Coulson, K.L., "Effect of Surface Reflection on the Angular and Spectral Distribution of Skylight," Journal of Atmospheric Sciences, Vol. 25, No. 5, 1968, pp. 759-770.
- Elterman, L., "UV, Visible and IR Attenuation for Altitudes to 50 km, 1968," Environmental Research Papers No. 285, Air Force Cambridge Research Laboratories, Bedford, Mass., 1968, 49 pp.
- Hovis, W.A., Private communication, 1971.
- Junge, C., "Gesetzmässigkeiten in der Grossenverteilung atmosphärischer Aerosol über dem Kontinent," Berichte Deutsche Wetterdienst U.S.-Zone, No. 35, 1952, pp. 261-277.
- Robinson, N., ed. Solar Radiation, Elsevier Publishing Co. New York, 1966, 347 pp.
- Salomonson, V.V., "Anisotropy in Reflected Solar Radiation," Atmospheric Science Paper No. 128, Colorado State University, Fort Collins, 1968, 143 pp.
- Thekaekara, M.P., "Proposed Standard Values of the Solar Constant and the Solar Spectrum," Journal of Environmental Sciences Vol 13, No. 4, 1970, pp. 6-9.
- Twomey, S., Jacobowitz, H., and Howell, H.B., "Matrix Method for Multiple-Scattering Problems," Journal of Atmospheric Sciences, Vol. 23, No. 3, 1966, pp. 289-296.

(Continued from inside front cover)

- NESS 57. Table of Scattering Function of Infrared Radiation for Water Clouds, Giichi Yamamoto, Masayuki Tanaka, and Shoji Asano, April 1971. (COM-71-50312)
- NESS 58. The Airborne ITPR Brassboard Experiment, W. L. Smith, D.T. Hilleary, E. C. Baldwin, W. Jacob, H. Jacobowitz, G. Nelson, S. Soules, D. Q. Wark, March 1972.
- NESS 59. Temperature Sounding From Satellites, S. Fritz, D. Q. Wark, H. E. Fleming, W. L. Smith, H. Jacobowitz, D. T. Hilleary, and J. C. Alishouse, July 1972.
- NESS 60. Satellite Measurements of Aerosol Backscattered Radiation From the Nimbus F Earth Radiation Budget Experiment, H. Jacobowitz, W. L. Smith, and A. J. Drummond, August 1972.
- NESS 61. The Measurement of Atmospheric Transmittance From Sun and Sky With an Infrared Vertical Sounder, W. L. Smith and H. B. Howell, September 1972.

PENN STATE UNIVERSITY LIBRARIES



A000072018323